ACCOUNTS
of chemical research

Construction of Homogenous/Heterogeneous Hollow Mesoporous Silica Nanostructures by Silica-Etching Chemistry: Principles, Synthesis, and Applications

YU CHEN, HANG-RONG CHEN,* AND JIAN-LIN SHI*

State Key Laboratory of High Performance Ceramics and Superfine Microstructures, Shanghai Institute of Ceramics, Chinese Academy of Sciences, Shanghai, 200050, P. R. China

RECEIVED ON MARCH 30, 2013

CONSPECTUS

Colloidal hollow mesoporous silica nanoparticles (HMSNs) are a special type of silica-based nanomaterials with penetrating mesopore channels on their shells. HMSNs exhibit unique structural characteristics useful for diverse applications: Firstly, the hollow interiors can function as reservoirs for enhanced loading of guest molecules, or as nanoreactors for the growth of nanocrystals or for catalysis in confined spaces. Secondly, the mesoporous silica shell enables the free diffusion of guest molecules through the intact shell. Thirdly, the outer silica surface is ready for chemical modifications, typically via its abundant Si−OH bonds.

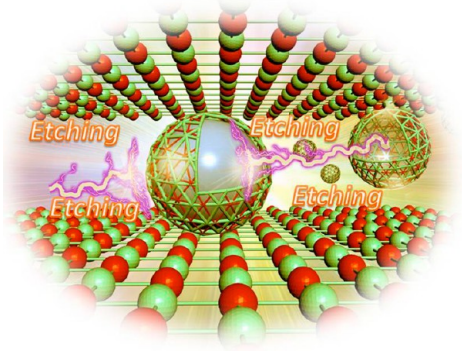

As early as 2003, researchers developed a soft-templating method to prepare hollow aluminosilicate spheres with penetrating mesopores in a cubic symmetry pattern on the shells. However, adapting this method for applications on the nanoscale, especially for biomedicine, has proved difficult because the soft templating micelles are very sensitive to liquid environments, making it difficult to tune key parameters such as dispersity, morphology and structure. In this Account, we present the most recent developments in the tailored construction of highly dispersive and monosized HMSNs using simple silica-etching chemistry, and we discuss these particles' excellent performance in diverse applications. We first introduce general principles of silica-etching chemistry for controlling the chemical composition and the structural parameters (particle size, pore size, etching modalities, yolk-shell nanostructures, etc.) of HMSNs. Secondly, we include recent progress in constructing heterogeneous, multifunctional, hollow mesoporous silica nanorattles via several methods for diverse applications. These elaborately designed HMSNs could be topologically transformed to prepare hollow mesoporous carbon nanoparticles or functionalized to produce HMSN-based composite nanomaterials. Especially in biomedicine, HMSNs are excellent as carriers to deliver either hydrophilic or hydrophobic anti-cancer drugs, to tumor cells, offering enhanced chemotherapeutic efficacy and diminished toxic side effects. Most recently, research has shown that loading one or more anticancer drugs into HMSNs can inhibit metastasis or reverse multidrug resistance of cancer cells. HMSNs could also deliver hydrophobic perfluorohexane (PFH) molecules to improve high intensity focused ultrasound (HIFU) cancer surgery by changing the tissue acoustic environment; and HMSNs could act as nanoreactors for enhanced catalytic activity and/or durability. The versatility of silica-etching chemistry, a simple but scalable synthetic methodology, offers great potential for the creation of new types of HMSN-based nanostructures in a range of applications.

1. Introduction

Hollow micro/nanostructural materials are a large family of functional materials with unique large hollow cavities, intact shells, and uniform morphologies, which endow them with great technological and scientific importance.[1] Among abundant hollow nanostructures, hollow mesoporous silica nanoparticles (HMSNs) have attracted the great attention due to their unique structural features and many corresponding interesting performances and applications.[2,3] In 2003, a typical soft-templating approach was proposed to prepare HMSNs with ordered mesoporous structures by using tetraethylorthosilicate (TEOS) emulsion as the

Published on the Web 08/14/2013 www.pubs.acs.org/accounts
10.1021/ar400091e

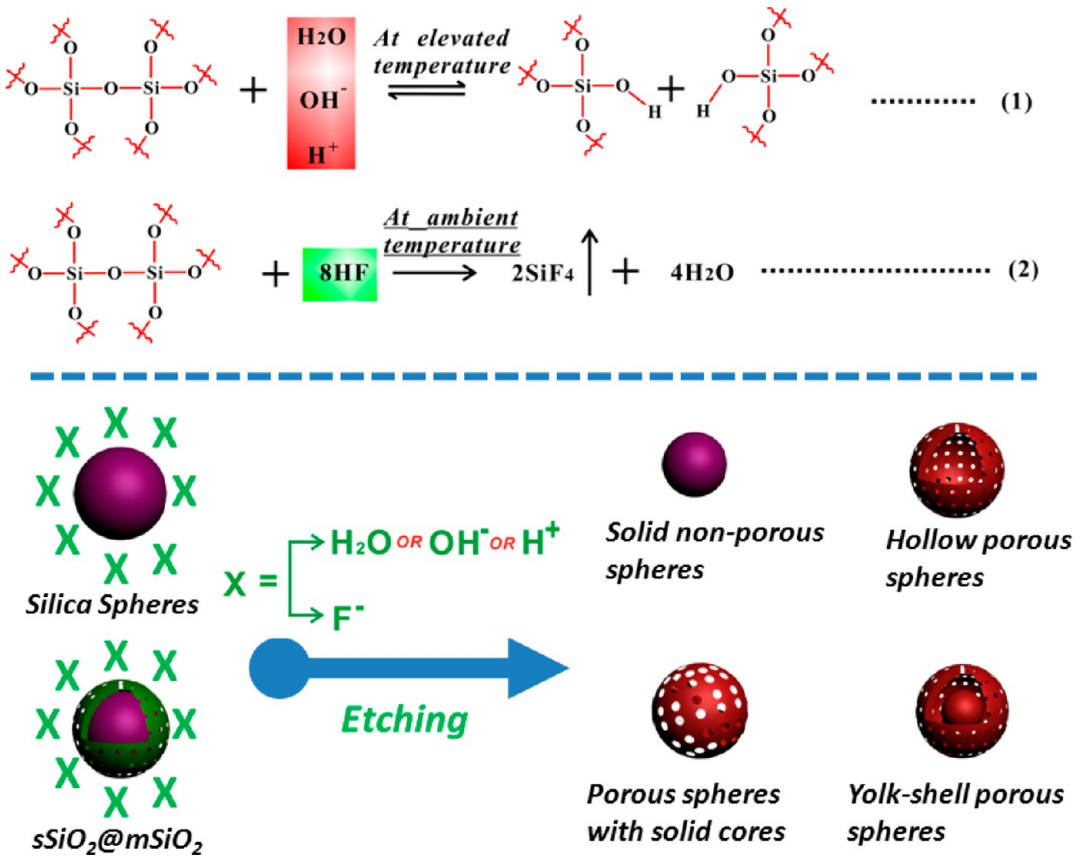

FIGURE 1. Schematic illustration of the simple silica-etching chemistry to tailor silica nanostructures.

self-template, that is, TEOS as oil droplets in water.[2] The obtained HMSNs exhibited substantially enhanced drug loading capacity compared to common mesoporous silica,[4] which is very suitable for drug transportations combined with the advantage that silica is "Generally Recognized As Safe" by the U.S. Food and Drug Administration. HMSNs were further modified by a special oppositely charged PAH/PSS polyelectrolyte multilayer to realize pH- and ion-strength-responsive drug release.[5] Unfortunately, these HMSNs were heavily aggregated and thus they could not satisfy the practical in vivo requirements.[2−5] It still remains a big challenge to fabricate well-defined and uniform HMSNs with tailored and desired compositions and nanostructures by typical soft-/hard-templating strategies.

Silica chemistry has been extensively applied in glass and ceramic fabrications, and it has also enlightened the importance of sol−gel chemistry in the large scale fabrication of advanced inorganic materials, mainly metal oxides involving silica nanomaterials, from initial chemical metal alkoxides to finial products. In addition to the general idea that silica chemistry is to progressively create a Si−O−Si network by hydrolysis and condensation reaction of chemical precursors dissolved in liquid media, the dissolution or breakage of Si−O−Si bond is the other opposite but important aspect of complex silica chemistry. This chemical essence is defined as the silica-etching chemistry, which has been extensively used for the removal of silica components in laboratory or industry. The typical etchants, such as hydrofluoric acid (HF) or alkaline substances (e.g., NaOH or ammonia) have been chosen to catalyze this reaction.

Typically, the silica-etching chemistry can be roughly divided into two categories (Figure 1): reversible etching in hot water/alkaline medium/strong acid solution and irreversible etching in HF solution. It is generally accepted that OH^- and F^- ions can etch amorphous silica framework by coordinating to Si atoms and breaking Si−O−Si bonds subsequently. Etching in hot water, alkaline medium (e.g., NaOH, Na_2CO_3, ammonia), or strong acid solution (e.g., HCl, H_2SO_4) includes the breakage of Si−O−Si bonds to form less condensed oligomers of silica species, which, however, can be chemically reversed by the bond formation among diverse preformed silicate oligomers. Comparatively, etching by HF is a very fast and irreversible process, and the main etched product is gaseous silicon tetrafluoride (SiF_4).[6−8] Recent results have demonstrated that this unique etching mechanism can generate diverse representative silica

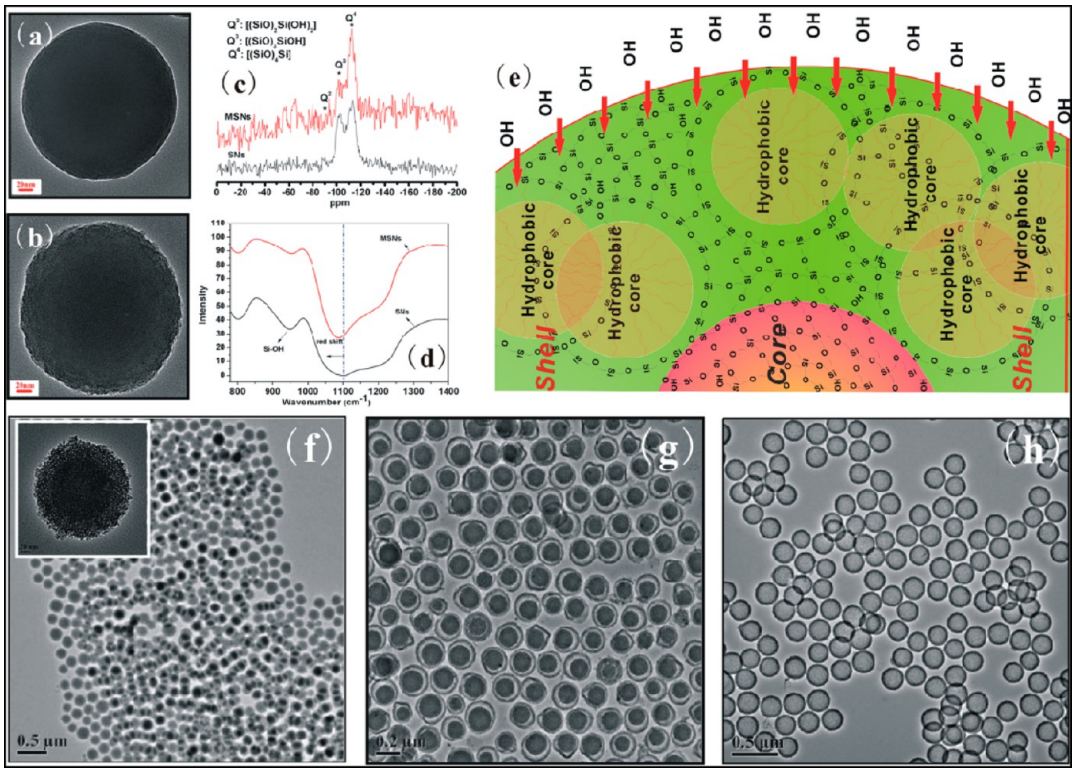

FIGURE 2. TEM images of a silica nanoparticle (a) and mesoporous silica nanoparticle (b). ^{29}Si NMR (c) and FTIR (d) spectra of SNs and MSNs. (e) Microstructure schematics of SiO_2@mSiO_2. TEM images of sSiO_2@mSiO_2 (f), yolk-shell (g), and hollow (h) MSNs. Reproduced with permission from ref 8. Copyright 2010 American Chemical Society.

nanostructures via varied etching processes provided that a special structural difference should be elaborately created in nanoparticulate systems, such as solid spheres with reduced sizes, hollow porous spheres, porous spheres with solid core and yolk-shell (rattle-type) porous spheres, and so forth.[9−13] The advantages of the silica-etching process in fabricating silica nanostructures lie in its simplicity and scalable feature, and the key structural parameters such as dimensions, dispersity and even mechanical property of the synthesized nanoparticles (NPs) can be well-controlled simply by adjusting the etching process or choosing adequate etchants.

Yin et al. successfully used NaOH to selectively etch the interior of silica spheres by using poly(vinyl pyrrolidone) protection on the surface of Stöber-based silica NPs.[9] They also found that $NaBH_4$ solution could directly transform silica NPs into rattle-type and hollow nanostructures by a dissolution-regrowth process.[10] Mou and co-workers successfully washed out the inner silica part of W/O reverse microemulsion-based silica NPs due to the less condensed inner silica section by organosilane incorporation.[11,12] Recently, Tang et al. synthesized a special sandwiched silica NPs, the middle layer of which was formed by the co-condensation between TEOS and *N*-[3-(trimethoxysilyl)propyl]ethylenediamine.[13] Interestingly, the organic/inorganic hybrid middle silica layer could be selectively removed by HF etching due to the less compact organic-silica framework. However, the etching-created mesoporosity in the shell was not well-defined and showed rather low surface area/pore volume. By understanding the essence and details of silica-etching chemistry, our recent results have demonstrated that such an etching mechanism could be directly used for precisely tailoring compositions, nanostructures and performances of HMSNs with well-defined mesoporous and hollow nanostructures. The premise of successful etching is to elaborately create a structural difference within a unique core/shell NPs between the solid silica core and the surfactant-templated mesoporous silica shell. In this Account, we describe the very recent progresses on the systematic construction and tailoring of the compositions and nanostructures of HMSNs by the silica-etching chemistry and their extensive applications in nanofabrication, nanobiomedicine, and nanocatalysis.

2. Design and Synthesis of HMSNs by Silica-Etching Chemistry and Their Characterizations

2.1. General Design Strategy and Preliminary Synthetic Results. Traditional hard-templating methodology employs

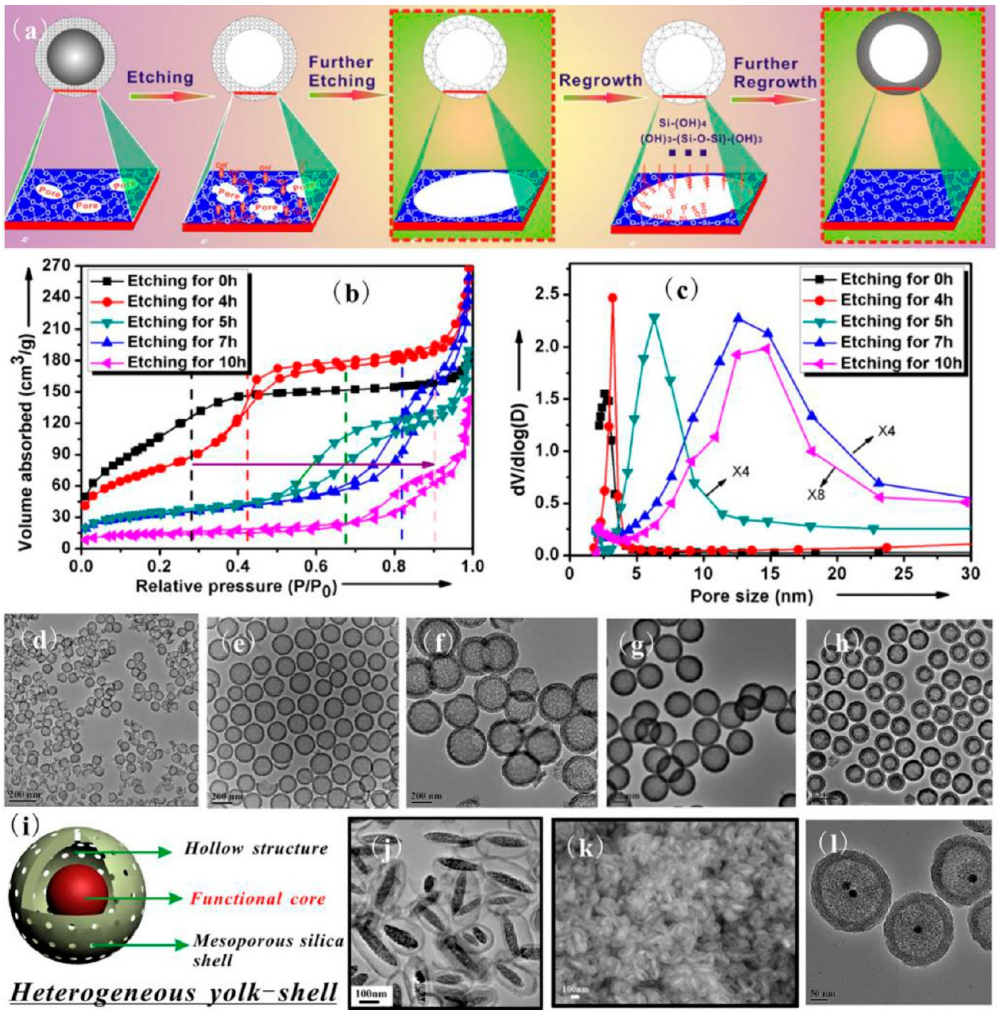

FIGURE 3. (a) Schematic illustration of etching process to tune the pore sizes of HMSNs; N_2 adsorption−desorption isotherms (b) and the corresponding pore size distributions (c) of HMSNs after etching for varied durations. Reproduced with permission from ref 17. Copyright 2011, Wiley-VCH Verlag GmbH & Co. KGaA, Weinheim. TEM images of HMSNs with different particle sizes (d, 70 nm; e, 180 nm; and f, 380 nm); TEM images of HMSNs obtained by HF etching (g) and H_2SO_4 etching (h); (i) structural illustration of multifunctionalized heterogeneous yolk-shell HMSNs; TEM (j) and SEM (k) images of Fe_3O_4@Void@mSiO_2; TEM image of Au@Void@mSiO_2 (l). Reproduced with permission frm ref 20. Copyright 2010 American Chemical Society.

the heterogeneous hard templates on which a layer of mesoporous silica layer is coated, and afterward the templates can be removed to leave a hollow interior. This is based on the compositional variations between the heterogeneous templating core and mesoporous silica shell.[1,14] Here presented etching strategy based on silica-etching chemistry is significantly different from traditional core/shell composition differences, but the structural differences with almost the same Si−O−Si compositions.

The most representative Si−O−Si composition-based NPs are traditional nonporous Stöber-based silica NPs (SNs, Figure 2a) and surfactant-templated mesoporous silica NPs (MSNs, Figure 2b).[8] Based on FTIR (Figure 2c) and ^{29}Si MAS NMR spectra (Figure 2d), it was found that the polymerization/condensation levels between SNs and MSNs were significantly different from each other. Octadecyltrimethoxysilane (C_{18}TMS)-directed MSNs showed higher condensation degrees compared to that of SNs. This was mainly due to the differences in the electrostatic/covalent interactions during the hydrolysis/condensation of silicon source under the absence/presence of pore-making agents. Then a distinctive core/shell structure with mesoporous silica as the shell and solid SNs as the core (sSiO_2@mSiO_2, Figure 2e and f) was easily produced by coating a mesoporous silica layer onto the surface of silica NPs prepared in advance. Thus, the structural differences between the core and shell were created for further etching without any supplementary step such as SNs' surface modification. Mesopore channels on the shells were then created simply by removing octadecyltrimethoxysilane (C_{18}TMS) which had been used to direct the

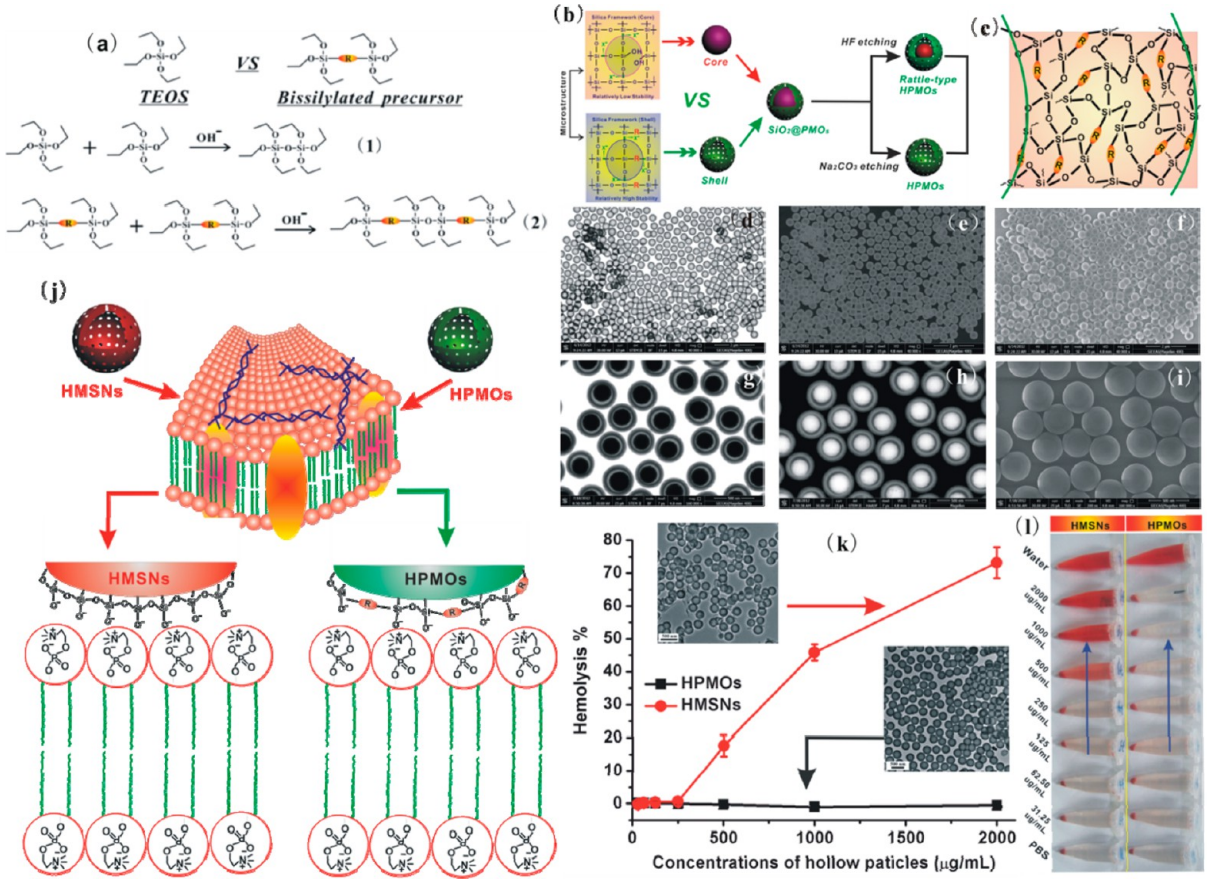

FIGURE 4. (a) Schematic illustration of the chemical homology between TEOS and bissilylated precursors for their hydrolysis and condensation under alkaline condition. (b) Synthetic scheme of HPMOs. (c) Microstructure of HPMOs' framework. Bright field (d, g), dark field (e, h), and second electron (f, i) images of HPMOs (d−f) and yolk-shell HPMOs (g−i) by SEM. (j) Schematics of the chemical interaction between the surface of HMSNs or HPMOs and cell membranes of RBCs. (k) Percentages of RBCs hemolysis after coincubation with HPMOs and HMSNs at different concentrations (inset: TEM images of HPMOs and HMSNs). (l) Digital photos showing the hemolytic effects after 2 h coincubation with HPMOs and HMSNs. Reproduced with permission from ref 7. Copyright 2013, Wiley-VCH Verlag GmbH & Co. KGaA, Weinheim.

formation of the mesosilica shell. Importantly, the SNs cores were easily etched away partially (Figure 2g) or completely (Figure 2h) to generate highly dispersed yolk-shell and hollow MSNs by either ammonia or Na_2CO_3 etching, respectively.[8] Comparatively, Zheng and co-workers proposed a special "cationic surfactant assisted selective etching" strategy to synthesize HMSNs with oriented mesoporous silica shell. It was found that cationic cetyltrimethyl ammonium bromide (CTAB) molecules can coassemble with etching-produced silicate species to reform the ordered mesoporous silica shell.[15,16] Monodispersed HMSNs with desired dimensions can be produced because Stöber method can generate monodispersed SNs as the cores with varied diameters. Besides, it is easy to achieve the coatings of mesoporous silica layers onto the silica cores with tunable thicknesses and the subsequent etching removal of the silica cores.

2.2. Key Structural Parameter Control and Core Functionalizations. The practical applications of HMSNs are highly dependent on their key structural parameters.[17,18] During the synthesis, it was found that the pore sizes could be tailored from 3.2 nm to larger than 10 nm under the etching with prolonged durations (Figure 3a−c).[17,18] Such a pore-expanding process includes etching $sSiO_2@mSiO_2$ to generate small pore-sized HMSNs and enlarging the pore sizes on the shells by fusing neighbor small pores together via Si−O−Si bond breakage under controlled etching conditions (Figure 3a). During the whole etching process, the shell skeleton keeps much less damaged due to the high condensation degrees.[17] Thanks to the mature Stöber process for the preparation of SNs cores, the particle size of HMSNs could be precisely tuned simply by changing the initial core diameter. For example, HMSNs with the particle sizes of about 70 nm (Figure 3d), 180 nm (Figure 3e), and 380 nm (Figure 3f) could be obtained without difficulties.

The etching modalities are also important to tune the key structural parameters of HMSNs. Although the alkaline

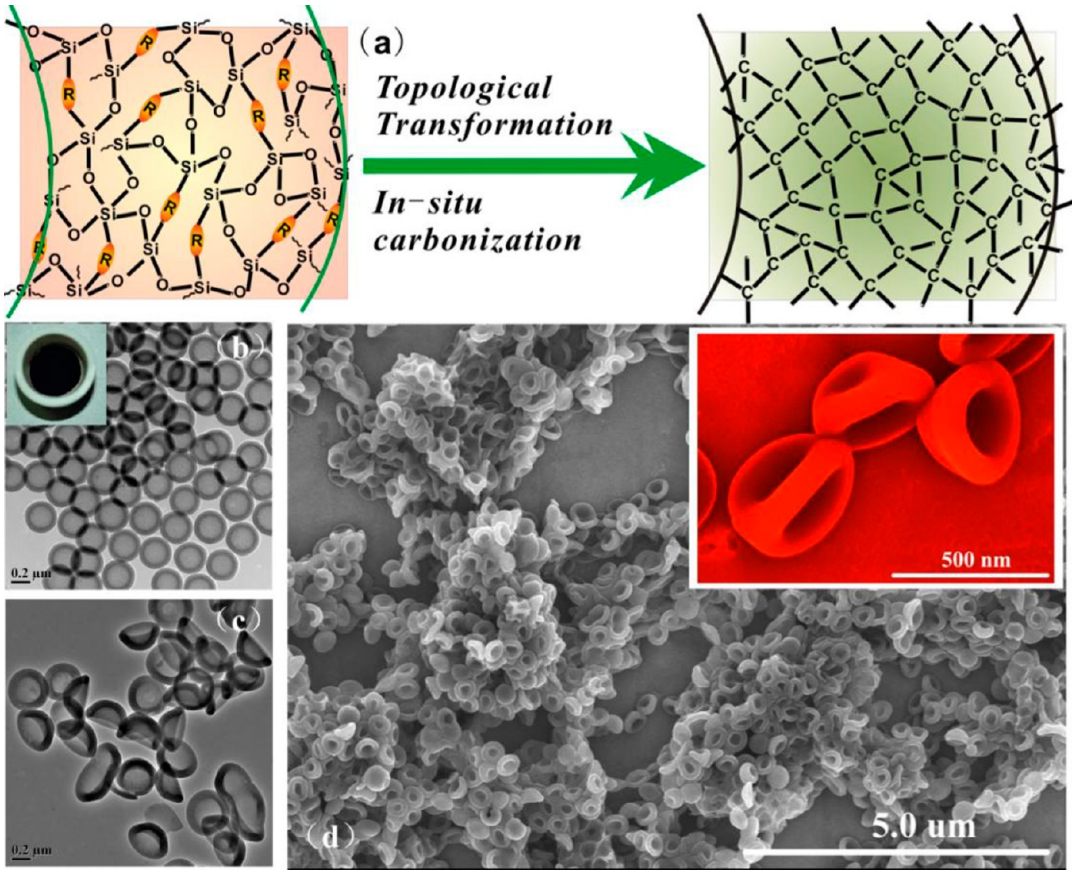

FIGURE 5. (a) Schematic illustration of topological transformation of HPMOs by carbonization under high temperature. TEM images of hollow SiO_2/C (b, inset: digital picture showing the carbonization of phenylene moieties) and HMCNs (c). (d) SEM image of HMCNs (inset: magnified SEM image showing the red blood cell-like morphology). Reproduced with permission from ref 7. Copyright 2013, Wiley-VCH Verlag GmbH & Co. KGaA, Weinheim.

etching can break the Si−O−Si bonds to form the hollow interiors (Na_2CO_3, ammonia, or NaOH),[6−11] such bond-breaking process is reversible accompanied with the simultaneous bound-reformation, which makes the etching process difficult to be controlled and brings with unexpected byproducts. A special fluoride-silica chemistry was further employed to prepare HMSNs by the chemical etching (Figure 3g).[6,13] Alternatively, the solid silica core of $sSiO_2@mSiO_2$ could also be etched away by strong acids (e.g., H_2SO_4, Figure 3h),[19] but the treatments at elevated temperatures and pressures are usually necessary in this etching process due to the relatively slow reaction kinetics.

This silica-etching process could be further employed to prepare heterogeneous yolk-shell multifunctional hollow nanostructures by further depositing mesoporous silica layers onto the surface of silica-coated nanocrystals ($M@SiO_2@mSiO_2$, M = Fe_2O_3, Fe_3O_4, Au, etc.) and subsequently etching away the middle silica layer (Figure 3i, $M@Void@mSiO_2$). By this synthetic strategy, $Fe_3O_4@Void@mSiO_2$[10,20−23] (Figure 3j and k) and $Au@Void@mSiO_2$[9,12,16,20] (Figure 3l) heterogeneous nanorattles were successfully fabricated.

2.3. Composition Control. It was further considered that the compositions of HMSNs are of equal significance because the composition modulations are expected to endow HMSNs with special biological features such as tunable biodegradation, improved biocompatibility, and even versatile functionality. As the representative organic−inorganic hybrid nanoporous materials, periodic mesoporous organosilicas (PMOs) with organic/inorganic components (silsesquioxane, $O_{1.5}Si−R−SiO_{1.5}$, R = organic groups) completely and homogeneously distributed within the framework are expected to find broad applications in nanotechnology. Typically, PMOs are formed by coassembly between hydrolyzed/condensed bissilylated precursors and surfactants/block copolymers, similar to synthesize traditional mesoporous silica materials.[3] Molecularly organic−inorganic hybrid HMSNs, that is, hollow PMO NPs (HPMOs), were successfully synthesized by silica-etching chemistry very recently.[7] Comparing the molecular structures between TEOS and bissilylated precursor (Figure 4a), it is found that there exists the chemical homology between them when they hydrolyze and condense to form pure

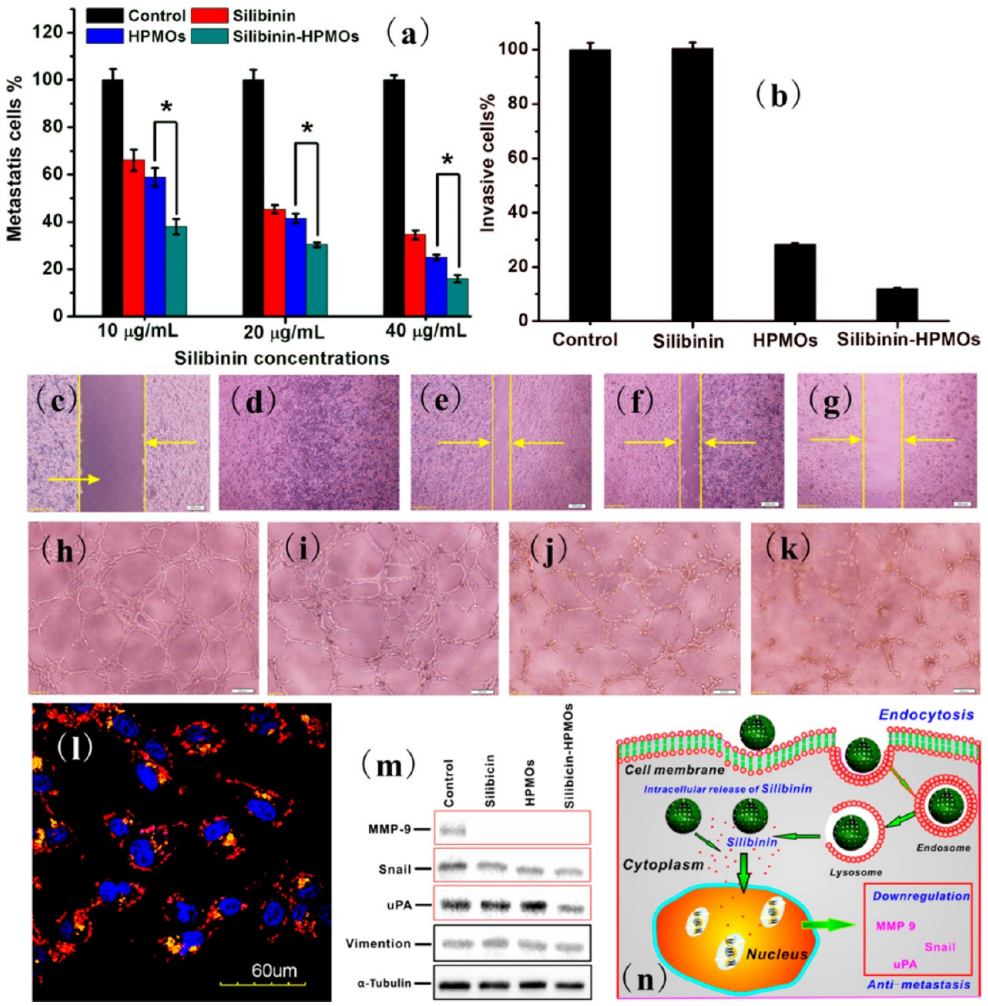

FIGURE 6. Percentages of migrated (a) and invasive (b, [silibinin] = 20 μg/mL) cells determined by the migration and invasion assays. Inhibition of migratory potential of MDA-MB-231 cancer cells by wound healing assay before (c) and after the different treatments (d, control; e, silibinin; f, HPMOs; and g, silibinin-HPMOs). Effect of introduction of free silibinin (i), HPMOs (j), and silibinin-HPMOs (k) on the capillary tube formation (figure h is the control). (l) CLSM images of MDA-MB-231 cancer cells after incubation with RITC-HPMOs for 2 h. (m) Inhibitory effects of free silibinin, HPMOs and silibinin-HPMOs on the expression of MMP-9, snail, uPA, Vimention, and α-tubulin obtained by Western blotting analysis. (n) Mechanism schematics of the intracellular delivery of silibinin by silibinin-loaded HPMOs and the antimetastasis effect against cancer cells. Reproduced with permission from ref 7. Copyright 2013, Wiley-VCH Verlag GmbH & Co. KGaA, Weinheim.

Si−O−Si and PMOs framework, respectively. Thus, a PMO layer can be easily deposited onto the surface of a silica NP to form SiO_2@PMOs with varied bissilylated precursors and without any surface modifications of SNs (Figure 4b and c).[7] It has been demonstrated that typical PMOs exhibit far higher chemical stability than MSNs with pure Si−O−Si frameworks, which indicates that Si−C−Si bond in PMOs is much more stable than Si−O−Si bond in silica under the presence of etchants. Thus, the silica core of SiO_2@PMOs can be etched away based on this structural difference by silica-etching chemistry while the PMO shell remains almost intact. Highly dispersed HPMOs (Figure 4d−f) and yolk-shell HPMOs (Figure 4g−i) were obtained by either Na_2CO_3 etching, ammonia or HF etching.[7] Due to the same chemical nature of hydrolysis/condensation of various bissilylated precursors, several HPMOs with diverse compositions (R = phenyl, ethyl, and vinyl groups) could also be fabricated based on etching process.[7]

The composition modulations can bring HMSNs with unique biological behaviors. For instance, the density of silanol groups on the surface of silica NPs is substantially reduced by the hybridization of phenylene groups and thus the hemolytic effect of HPMOs is significantly lower than that of traditional HMSNs (Figure 4j).[7] Even at the extremely high concentration of 2000 μg/mL where the hemolysis percentage of HMSNs reached 73.2%, no significant hemolysis effect was observed upon the exposure of red blood cells (RBCs) to HPMOs at the same concentration (Figure 4k and l).

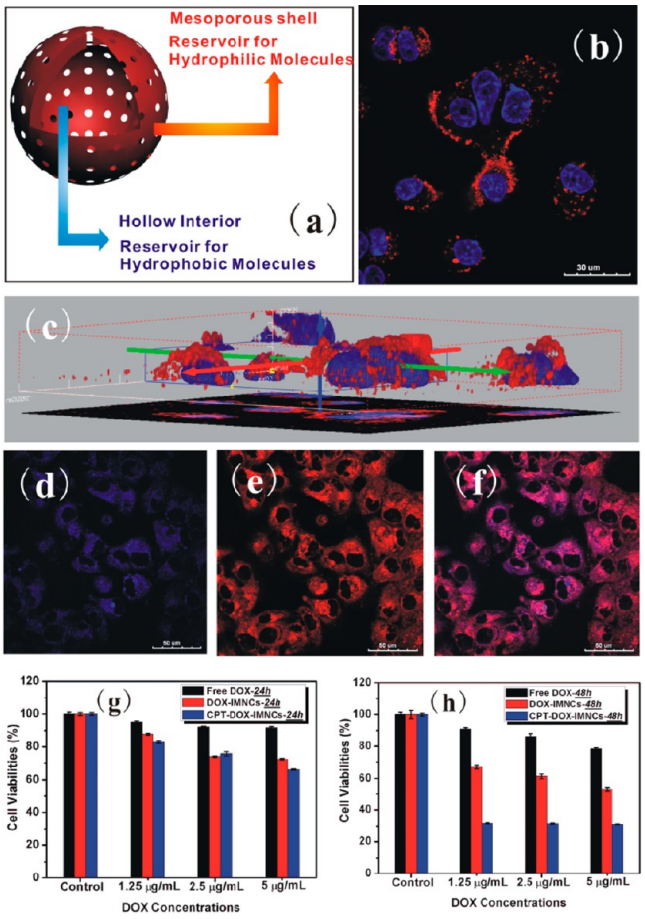

FIGURE 7. (a) Schematic illustration of HMSNs for the coloading of hydrophilic and hydrophobic agents. (b) CLSM image of MCF-7/ADR cells after coincubation with RhB-HMSNs. (c) 3D confocal fluorescence reconstruction of HMSNs-endocytosed MCF-7/ADR cells. CLSM images of MCF-7/ADR cells after incubation with DOX and CPT double-loaded HMSNs (d, CPT; e, DOX; and f, merged image). Cell viabilities of free DOX, DOX-HMSNs and DOX/CPT-HMSNs against MCF-7/ADR for different time intervals (g, 24 h and h, 48 h). Reproduced with permission from ref 6. Copyright 2012, Wiley-VCH Verlag GmbH & Co. KGaA, Weinheim.

Long-term in vivo histocompatibility assay further demonstrated the high biocompatibility of HPMOs.[7]

3. Applications of HMSNs

3.1. Nanofabrication. HMSNs with diverse particle/pore sizes and compositions provide an excellent platform for nanofabrication, which means that other functional NPs can be fabricated by direct framework transformation or functionalization of HMSNs. It was demonstrated that the phenylene-hybrid HPMOs could be directly carbonized to generate carbon framework within the silica framework at molecular scale.[7] New types of uniform hollow silica/carbon (SiO_2/C) composite NPs (Figure 5a and b) and hollow mesoporous carbonaceous nanocapsules (HMCNs, Figure 5c and d) could be facilely synthesized by removing the silica moieties present within the framework.

The well-defined mesoporosity provides useful mesopore channels for in situ growth of NPs within them. Moreover, the large hollow interiors can be used for the preparation of heterogeneous functional nanorattles, and the abundant surface chemistry makes the surface engineering possible, such as PEGylation or targeting modifications. Therefore, a large family of HMSNs-based multifunctional NPs with tailored functionalities can be achieved by advanced nanosynthetic chemistry.[1,8−10,12,16,20,24]

3.2. Drug Delivery. MSNs have been extensively explored for biomedical applications.[25−31] Comparatively, HMSNs are more suitable for drug delivery due to the presence of large hollow interiors, which leave large room for drug molecule encapsulation with extraordinarily high drug loading capacity.[4,8] However, only the applications of HMSNs or HMPOs as drug carriers in antimetastasis and multidrug resistance reversing of cancer cells will be discussed here in detail.

Lu's group found that HPMOs exhibited higher drug (antibiotic tetracycline)-loading capacity and slower release rate compared to traditional MSNs and PMOs without hollow nanostructures.[32] Recently, an antimetastasis hydrophobic drug (silibinin) was encapsulated into HPMOs to evaluate their performances in antimetastasis of cancer cells.[7] The drug loading amount could reach 143.8 mg/g and the release profile showed a sustained pattern. The antimigration (Figure 6a), anti-invasion (Figure 6b), antiwound healing (Figure 6c−g), and antiangiogenesis (Figure 6h−k) assays demonstrated that the metastasis of MDA-MB-231 cancer cells could be strongly inhibited by the introduction of silibinin-HPMOs, and the formation of capillary tubes and cellular network structures of human microvascular endothelial cells (HMEC) was notably inhibited. Based on confocal laser scanning microscopy (CLSM) observations (Figure 6l) and western-blotting analysis (Figure 6m), it was deduced that the hydrophobic silibinin molecules can be transported into cancer cells mediated by HPMOs via a typical endocytosis process to silence the expression of main proteins related to the metastasis of cancer cells, such as MMP-9, Snail and uPA, and thus the metastasis of cancer cells can be remarkably inhibited or even prevented (Figure 6n).[7]

In addition to the efficient encapsulation of hydrophobic anticancer agents within the hollow interiors in as early as 2005,[5] the well-defined mesopores within the shell can be further used for the loading of hydrophilic drug molecules (Figure 7a).[6] The coloading of drugs can bring with synergistic therapeutic outcomes, especially for reversing the multidrug resistance (MDR) of cancer cells. It was found that doxorubicin (DOX)-resistant MCF-7/ADR cancer cells could

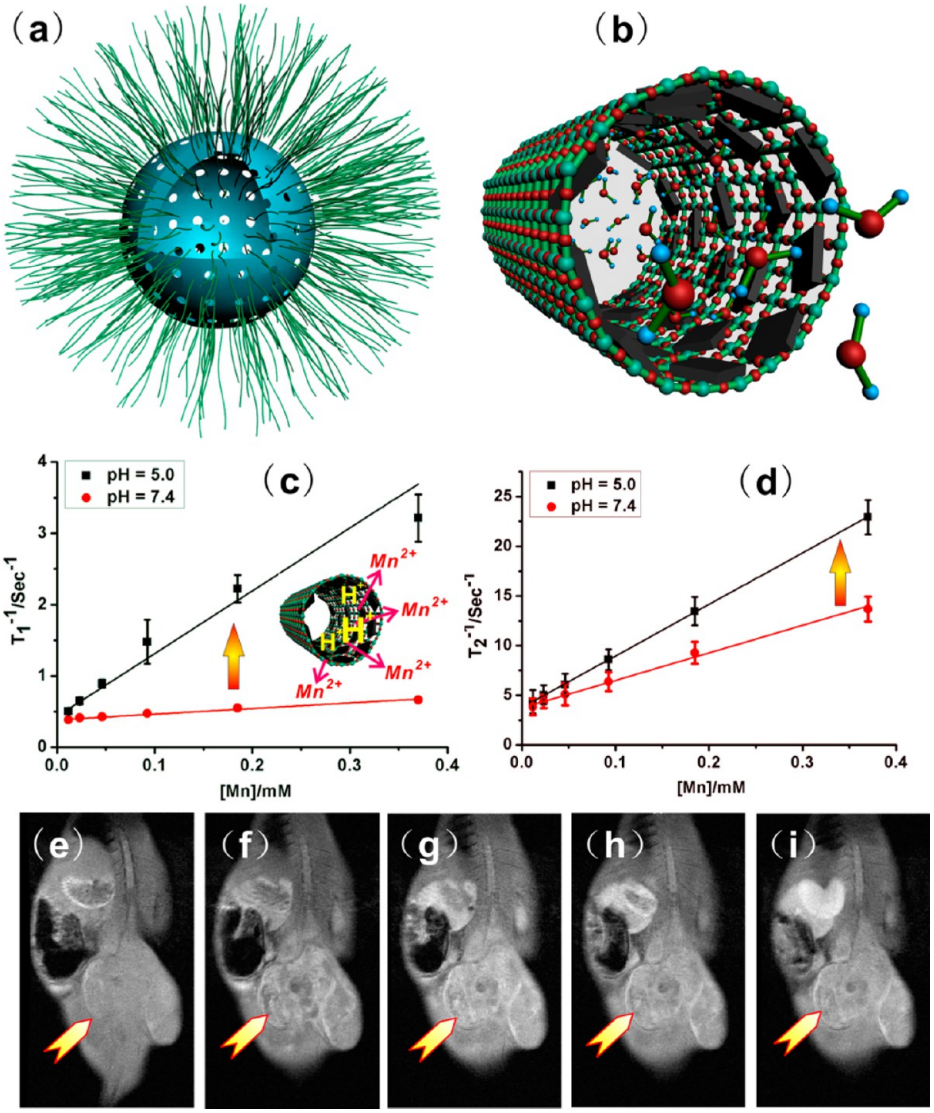

FIGURE 8. Schematic illustration of PEGylated MnOx/HMSNs (a) and the inner microstructure of mesopores after MnOx decoration (b). T_1 (c) and T_2 (d) relaxivities of the aqueous suspensions of MnOx/HMSNs after 4 h soaking in buffer solutions of different pH values (7.4 and 5.0) at 37 °C. In vivo T_1-weighted MRI of tumor before (e) and after intravenous administration of HMCNs (f, 5 min; g, 15 min; h, 30 min; and i, 60 min; arrows indicate the tumor tissue). Reproduced with permission from refs 33 and 34. Copyright 2012, Elsevier.

uptake HMSNs with high efficiency by CLSM observations (Figure 7b and c). By further coloading hydrophilic DOX and hydrophobic camptothecin (CPT) within HMSNs, it was found that the codelivery of dual drug combinations enabled the intracellular delivery and release of two anticancer agents (Figure 7d–f), which resulted in enhanced therapeutic effects for DOX-resistant MCF-7/ADR cancer cells (Figure 7g and h) by MTT assay.

3.3. As Contrast Agents for Molecular Imaging. The functionalization of HMSNs can endow them with the capability of molecular imaging, and thus, they can be used as the theranostic agents for simultaneous diagnosis and therapy. For instance, magnetic Fe_3O_4 NPs-encapsulated HMSNs (Fe_3O_4@Void@mSiO_2 heterogeneous nanorattles) can function as the contrast agents for T_2-weighted magnetic resonance imaging (MRI),[20−22] and the Au core in Au@Void@mSiO_2 can be used for dark-field light scattering cell labeling due to the surface plasma resonance effect of Au NPs.[20]

Recently, MnOx NPs were introduced within the mesopore channels of HMSNs by an in situ redox reaction between structure-directing agents and $KMnO_4$.[33,34] This strategy could disperse the manganese paramagnetic center within mesopores to a remarkably high extent, by which the chances of interaction between water molecules and manganese centers were greatly boosted (Figure 8a and b). As a result, the T_1-weighted MRI performance could be

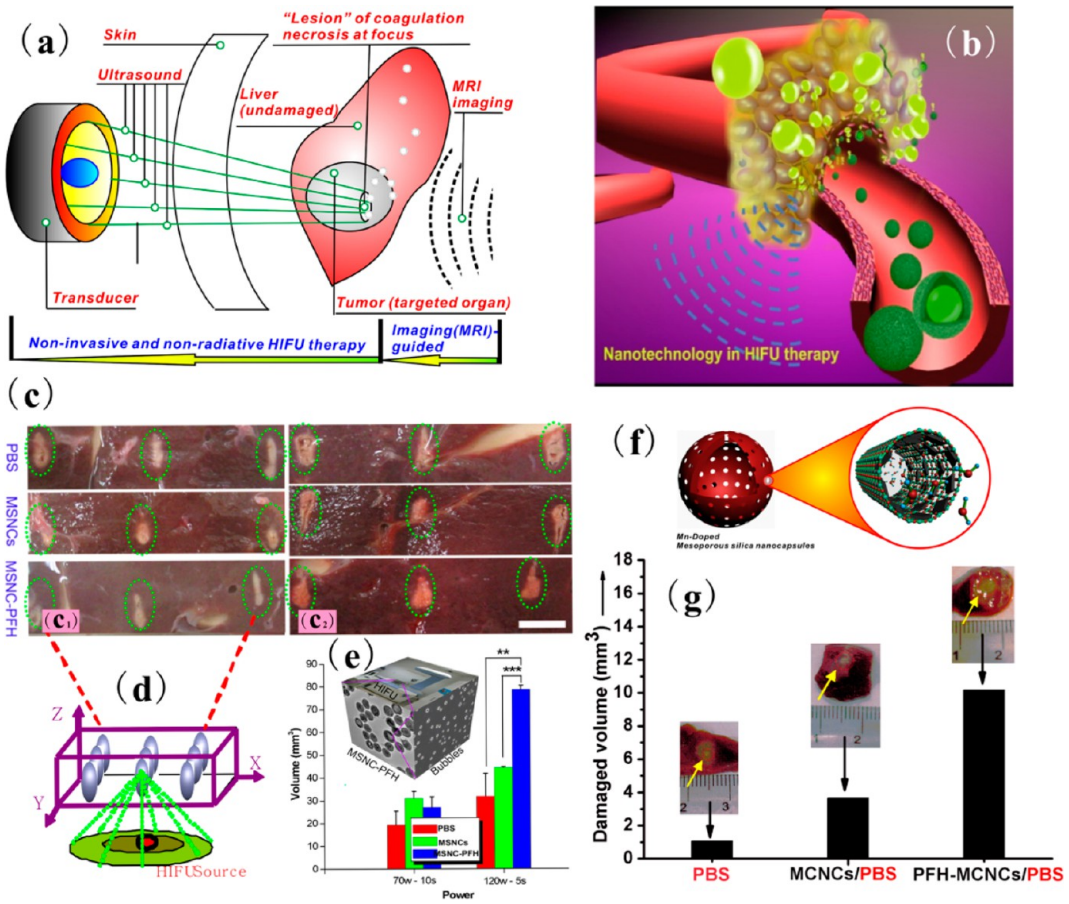

FIGURE 9. (a) Technical principle of MRI-guided HIFU for the surgery of hepatic neoplasm in rabbits. (b) Scheme of PFH-HMSNs transportation within blood vessels. Digital photos (c) of ablated bovine livers at (c_1) 70 W/cm^2 for 10 s, (c_2) 120 W/cm^2 for 5 s, and (e) the corresponding necrotic volume after being injected of 3 mL PBS control, HMSNs, and PFH-HMSNs, respectively (d is the schematic 3D illustration of ablated process on bovine livers ex vivo). (f) Schematic illustration of MnOx/HMSNs for HIFU therapy. (g) In vivo coagulated necrotic tumor volume by MRI-guided HIFU exposure under the irradiation power of 150 W/cm^2 and duration of 5 s in rabbit liver tumors after receiving different agents via ear vein. Reproduced with permission from refs 35 and 36. Copyright 2012 and 2011, Wiley-VCH Verlag GmbH & Co. KGaA, Weinheim.

substantially improved. Importantly, these MnOx NPs exhibit acid-induced dissolution behavior, by which the dissolved Mn^{2+} ion possesses the highest chances to interaction with water molecules. Therefore, MnOx/HMSNs exhibited an interesting pH-dependent dynamic MRI behavior. It was found that the relaxation rate r_1 of MnOx/HMSNs in the low pH solution (Figure 8c and d, pH = 5.0, r_1 = 8.81 mM^{-1} s^{-1}) increased significantly compared to those in the high pH one (pH = 7.0, r_1 = 0.79 mM^{-1} s^{-1}), which was substantially higher than that of commercial Gd^{III}-based small molecular chelates (e.g., Magnevist ($r_1 \approx 3.4$ mM^{-1} s^{-1})). In vivo MRI assay indicated that the MnOx/HMSNs showed T_1-weighted positive contrast-enhanced MR imaging capability for tumor tissues after intravenous administration due to the enhanced permeability and retention effect (Figure 8e and f). The tumor tissue exhibited strong T_1 contrast enhancements gradually in the time course (Figure 8g–i), which was attributed to the leaching out of manganese ions responsible for the enhanced T_1-weighted MRI performances under the weak acidic tumor microenvironment, further indicating that MnOx/HMSNs could be used as manganese ion-delivery vehicles for the in vivo pH-sensitive tumor imaging.

3.4. HIFU Synergistic Therapy for Cancer Surgery. Recently, HMSNs were employed as carriers for the delivery of hydrophobic perfluorohexane (PFH), which function as the synergistic agents (SAs) for enhanced high intensity focused ultrasound (HIFU) cancer surgery.[6,35] Ultrasound can be focused on the in vivo target tissue under the guidance by various imaging modalities (ultrasonography or MRI, Figure 9a). The PFH-loaded HMSNs could transport into tumor tissues through blood vessels, and they played a role of synergistic therapy upon HIFU irradiation (Figure 9b). The hydrophobic PFH-loaded HMSNs could be well-dispersed in water, and the evaporation process of PFH from HMSNs

under elevated temperatures could be monitored and observed by CLSM.[35] The introduced PFH-HMSNs significantly enhanced the HIFU therapeutic outcome as reflected by the enlarged damaged bovine liver volumes ex vivo (Figure 9c–e) due to the change of tissue acoustic environment.[6,35]

Furthermore, MnOx NPs were decorated within the mesopores of HMSNs (designated as PFH-MCNCs) to endow them with T_1-weighted MRI capabilities (Figure 9f), which was further employed for MRI-guided HIFU cancer surgery.[36] After the intravenous administration of PFH-MCNCs into rabbits bearing VX2 liver tumor via ear vein, the T_1-weighted MRI showed that the signals of liver increased significantly in the prolonged time course, by which the boundary between tumor and normal tissue could be distinguished clearly. The ex vivo and in vivo synergistic effect assessment further demonstrated the enhanced therapeutic efficacy by the introduction of PFH-MCNCs (Figure 9g). The mean volume of tumor coagulation by HIFU irradiation in the rabbits received PFH-MCNCs (10.2 mm^3) is 8.3 and 1.8 times larger than in the rabbits received only PBS (1.1 mm^3) and MnOx/HMSNs (3.7 mm^3), respectively. Very recently, it was found that the decoration of Au NPs onto the surface of HMSNs could further enhance the HIFU therapeutic efficiency compared to blank HMSNs due to their high thermal conductivity.[37] It is believed that this work will be potentially but highly promising for introducing nanobiotechnology in enhancing the therapeutic efficacy of special therapeutic modalities in clinics, such as HIFU surgery, radiation treatment, microwave therapy, radiofrequency therapy, and so forth, in future.

3.5. As Nanoreactors for Nanocatalytic Applications. The unique structure of HMSNs provides an excellent platform for nanocatalytic applications.[38,39] The large hollow interior can be used as nanoreactors for active species and the well-defined mesoporous shell provides the diffusion pathways for reactants or products. For heterogeneous yolk-shell M@Void@mSiO_2, the mesoporous silica shell can prevent the functional cores from growth and/or agglomeration with each other during the catalytic reactions to guarantee the reproducibility and recyclability of the catalysts, especially for the reactions at elevated temperatures.

Several reports have demonstrated the catalytic applications of silica etching-synthesized nanostructures. Yin et al.,[9] Mou et al.,[12] and Zheng et al.[16] have demonstrated that Au@Void@mSiO_2 showed excellent catalytic activity and recyclability for the reduction of 4-nitrophenol compared with bare Au NPs. Lu et al. demonstrated that Pd@Void@HP-MOs nanorattles exhibited high conversion (~100%) and excellent selectivity (~99%) toward selective oxidation of alcohols to aldehydes.[40] In addition, active species with different functions can be introduced within the separate parts of HMSNs, such as acidic active center within mesoporous silica shell and basic active center within the heterogeneous core,[41] which means that modified or doped HMSNs can function as the multifunctional catalysts for different chemical reactions.

4. Conclusions and Prospects

The unique structural characteristics of HMSNs have made them highly useful in nanofabrication, nano-biomedicine, and nanocatalysis. The exploration of simple and economic synthetic methodology will greatly favor their large-scale applications in future. By simple silica-etching chemistry, the well-defined and monodispersed homogeneous/heterogeneous HMSNs with varied particle/pore sizes, compositions, and functionalities could be successfully fabricated in a large-scale manner.

In addition to the diverse HMSNs described in this Account, there is still large space for synthesizing other types of HMSN-based nanostructures based on the silica-etching chemistry. For biomedical applications, the composition should be further tailored to endow HMSNs with enhanced biosafety, such as tunable biodegradability and diminished toxic side effects. Moreover, it is still a big challenge to prepare HMSNs simultaneously with smaller particle sizes less than, for example, 100 nm and large enough pores (e.g., >10 nm) by silica-etching process, while these special HMSNs are of great significance for in vivo delivery of large biomolecules such as siRNA or DNA. The exact mechanisms involved in silica-etching chemistry should be further clarified to provide more exact theoretical foundation for tailoring the nanostructures of silica. In fact, the concepts and methods presented in this Account, including the versatile silica-etching processes based on the structural differences to prepare HMSNs, can be applied to other material systems involving etching processes to produce NPs with desired compositions and nanostructures, especially with hollow nanostructures.

This work was supported by the National Nature Science Foundation of China (Grant No. 51132009, 51072212), the National Basic Research Program of China (973 Program, Grant No. 2011CB707905), China National Funds for Distinguished Young Scientists (Grant No.51225202), Nano special program of the Science and Technology Commission of Shanghai (Grant No. 11 nm0506500), and Foundation for Youth Scholar of State Key Laboratory of High Performance Ceramics and Superfine Microstructures (Grant No. SKL201203).

BIOGRAPHICAL INFORMATION

Yu Chen received his Ph.D. degree from Shanghai Institute of Ceramics, Chinese Academy of Sciences (SICCAS) in 2012. He is now assistant professor in SICCAS. His research is focused on the design, synthesis, and nanobiomedical applications of multifunctional mesoporous materials.

Hang-Rong Chen received her Ph.D. degree from SICCAS. She is a full professor and Ph.D. supervisor in SICCAS since 2006. Her recent research interest focuses on nanoscale materials with novel mesopores and/or specific structures as drug delivery systems of controlled drug release.

Jian-Lin Shi received his Ph.D. degree from SICCAS. He is now full professor of SICCAS and the director of the State Key Lab of High Performance Ceramics and Superfine Microstructure. His research areas include synthesis of mesoporous materials and mesoporous-based nanocomposites, and their catalytic, biomedical, and optical applications. He has published over 300 scientific papers which have been cited more than 7800 times by other scientists with an h-index of 43 (2012).

FOOTNOTES

*To whom correspondence should be addressed. E-mail: jlshi@sunm.shcnc.ac.cn (J.S.); hrchen@mail.sic.ac.cn (H.C.).

The authors declare no competing financial interest.

REFERENCES

1 Lou, X. W.; Archer, L. A.; Yang, Z. C. Hollow Micro-/Nanostructures: Synthesis and Applications. *Adv. Mater.* **2008**, *20*, 3987–4019.

2 Li, Y. S.; Shi, J. L.; Hua, Z. L.; Chen, H. R.; Ruan, M. L.; Yan, D. S. Hollow spheres of mesoporous aluminosilicate with a three-dimensional pore network and extraordinarily high hydrothermal stability. *Nano Lett.* **2003**, *3*, 609–612.

3 Djojoputro, H.; Zhou, X. F.; Qiao, S. Z.; Wang, L. Z.; Yu, C. Z.; Lu, G. Q. Periodic mesoporous organosilica hollow spheres with tunable wall thickness. *J. Am. Chem. Soc.* **2006**, *128*, 6320–6321.

4 Zhu, Y. F.; Shi, J. L.; Chen, H. R.; Shen, W. H.; Dong, X. P. A facile method to synthesize novel hollow mesoporous silica spheres and advanced storage property. *Microporous Mesoporous Mater.* **2005**, *84*, 218–222.

5 Zhu, Y. F.; Shi, J. L.; Shen, W. H.; Dong, X. P.; Feng, J. W.; Ruan, M. L.; Li, Y. S. Stimuli-responsive controlled drug release from a hollow mesoporous silica sphere/polyelectrolyte multilayer core-shell structure. *Angew. Chem., Int. Ed.* **2005**, *44*, 5083–5087.

6 Chen, Y.; Gao, Y.; Chen, H. R.; Zeng, D. P.; Li, Y. P.; Zheng, Y. Y.; Li, F. Q.; Ji, X. F.; Wang, X.; Chen, F.; He, Q. J.; Zhang, L. L.; Shi, J. L. Engineering Inorganic Nanoemulsions/Nanoliposomes by Fluoride-Silica Chemistry for Efficient Delivery/Co-Delivery of Hydrophobic Agents. *Adv. Funct. Mater.* **2012**, *22*, 1586–1597.

7 Chen, Y.; Xu, P.; Chen, H.; Li, Y.; Bu, W.; Shu, Z.; Li, Y.; Zhang, J.; Zhang, L.; Pan, L.; Cui, X.; Hua, Z.; Wang, J.; Zhang, L.; Shi, J. Colloidal HPMO Nanoparticles: Silica-Etching Chemistry Tailoring, Topological Transformation, and Nano-Biomedical Applications. *Adv. Mater.* **2013**, *25*, 3100–3105.

8 Chen, Y.; Chen, H. R.; Guo, L. M.; He, Q. J.; Chen, F.; Zhou, J.; Feng, J. W.; Shi, J. L. Hollow/Rattle-Type Mesoporous Nanostructures by a Structural Difference-Based Selective Etching Strategy. *ACS Nano* **2010**, *4*, 529–539.

9 Zhang, Q.; Zhang, T. R.; Ge, J. P.; Yin, Y. D. Permeable silica shell through surface-protected etching. *Nano Lett.* **2008**, *8*, 2867–2871.

10 Zhang, T. R.; Ge, J. P.; Hu, Y. X.; Zhang, Q.; Aloni, S.; Yin, Y. D. Formation of hollow silica colloids through a spontaneous dissolution-regrowth process. *Angew. Chem., Int. Ed.* **2008**, *47*, 5806–5811.

11 Lin, Y. S.; Wu, S. H.; Tseng, C. T.; Hung, Y.; Chang, C.; Mou, C. Y. Synthesis of hollow silica nanospheres with a microemulsion as the template. *Chem. Commun.* **2009**, 3542–3544.

12 Wu, S. H.; Tseng, C. T.; Lin, Y. S.; Lin, C. H.; Hung, Y.; Mou, C. Y. Catalytic nano-rattle of Au@hollow silica: towards a poison-resistant nanocatalyst. *J. Mater. Chem.* **2011**, *21*, 789–794.

13 Chen, D.; Li, L. L.; Tang, F. Q.; Qi, S. O. Facile and Scalable Synthesis of Tailored Silica "Nanorattle" Structures. *Adv. Mater.* **2009**, *21*, 3804–3807.

14 Caruso, F.; Caruso, R. A.; Mohwald, H. Nanoengineering of inorganic and hybrid hollow spheres by colloidal templating. *Science* **1998**, *282*, 1111–1114.

15 Fang, X. L.; Chen, C.; Liu, Z. H.; Liu, P. X.; Zheng, N. F. A cationic surfactant assisted selective etching strategy to hollow mesoporous silica spheres. *Nanoscale* **2011**, *3*, 1632–1639.

16 Fang, X. L.; Liu, Z. H.; Hsieh, M. F.; Chen, M.; Liu, P. X.; Chen, C.; Zheng, N. F. Hollow Mesoporous Aluminosilica Spheres with Perpendicular Pore Channels as Catalytic Nanoreactors. *ACS Nano* **2012**, *6*, 4434–4444.

17 Chen, Y.; Chu, C.; Zhou, Y. C.; Ru, Y. F.; Chen, H. R.; Chen, F.; He, Q. J.; Zhang, Y. L.; Zhang, L. L.; Shi, J. L. Reversible Pore-Structure Evolution in Hollow Silica Nanocapsules: Large Pores for siRNA Delivery and Nanoparticle Collecting. *Small* **2011**, *7*, 2935–2944.

18 Gao, Y.; Chen, Y.; Ji, X. F.; He, X. Y.; Yin, Q.; Zhang, Z. W.; Shi, J. L.; Li, Y. P. Controlled Intracellular Release of Doxorubicin in Multidrug-Resistant Cancer Cells by Tuning the Shell-Pore Sizes of Mesoporous Silica Nanoparticles. *ACS Nano* **2011**, *5*, 9788–9798.

19 Yu, Q. Y.; Wang, P. P.; Hu, S.; Hui, J. F.; Zhuang, J.; Wang, X. Hydrothermal Synthesis of Hollow Silica Spheres under Acidic Conditions. *Langmuir* **2011**, *27*, 7185–7191.

20 Chen, Y.; Chen, H. R.; Zeng, D. P.; Tian, Y. B.; Chen, F.; Feng, J. W.; Shi, J. L. Core/Shell Structured Hollow Mesoporous Nanocapsules: A Potential Platform for Simultaneous Cell Imaging and Anticancer Drug Delivery. *ACS Nano* **2010**, *4*, 6001–6013.

21 Chen, Y.; Chen, H. R.; Zhang, S. J.; Chen, F.; Zhang, L. X.; Zhang, J. M.; Zhu, M.; Wu, H. X.; Guo, L. M.; Feng, J. W.; Shi, J. L. Multifunctional Mesoporous Nanoellipsoids for Biological Bimodal Imaging and Magnetically Targeted Delivery of Anticancer Drugs. *Adv. Funct. Mater.* **2011**, *21*, 270–278.

22 Wu, H. X.; Zhang, S. J.; Zhang, J. M.; Liu, G.; Shi, J. L.; Zhang, L. X.; Cui, X. Z.; Ruan, M. L.; He, Q. J.; Bu, W. B. A Hollow-Core, Magnetic, and Mesoporous Double-Shell Nanostructure: In Situ Decomposition/Reduction Synthesis, Bioimaging, and Drug-Delivery Properties. *Adv. Funct. Mater.* **2011**, *21*, 1850–1862.

23 Zhao, W. R.; Chen, H. R.; Li, Y. S.; Li, L.; Lang, M. D.; Shi, J. L. Uniform Rattle-type Hollow Magnetic Mesoporous Spheres as Drug Delivery Carriers and their Sustained-Release Property. *Adv. Funct. Mater.* **2008**, *18*, 2780–2788.

24 Guo, L. M.; Li, J. T.; Zhang, L. X.; Li, J. B.; Li, Y. S.; Yu, C. C.; Shi, J. L.; Ruan, M. L.; Feng, J. W. A facile route to synthesize magnetic particles within hollow mesoporous spheres and their performance as separable Hg^{2+} adsorbents. *J. Mater. Chem.* **2008**, *18*, 2733–2738.

25 Wu, S. H.; Mou, C. Y.; Lin, H. P. Synthesis of mesoporous silica nanoparticles. *Chem. Soc. Rev.* **2013**, *42*, 3862–3875.

26 Liu, J.; Qiao, S. Z.; Hartono, S. B.; Lu, G. Q. Monodisperse Yolk-Shell Nanoparticles with a Hierarchical Porous Structure for Delivery Vehicles and Nanoreactors. *Angew. Chem., Int. Ed.* **2010**, *49*, 4981–4985.

27 Liu, J.; Bu, W.; Pan, L.; Shi, J. NIR-Triggered Anticancer Drug Delivery by Upconverting Nanoparticles with Integrated Azobenzene-Modified Mesoporous Silica. *Angew. Chem., Int. Ed.* **2013**, *52*, 4375–4379.

28 Niu, D. C.; Ma, Z.; Li, Y. S.; Shi, J. L. Synthesis of Core-Shell Structured Dual-Mesoporous Silica Spheres with Tunable Pore Size and Controllable Shell Thickness. *J. Am. Chem. Soc.* **2010**, *132*, 15144–15147.

29 Pan, L. M.; He, Q. J.; Liu, J. N.; Chen, Y.; Ma, M.; Zhang, L. L.; Shi, J. L. Nuclear-Targeted Drug Delivery of TAT Peptide-Conjugated Monodisperse Mesoporous Silica Nanoparticles. *J. Am. Chem. Soc.* **2012**, *134*, 5722–5725.

30 Tarn, D.; Ashley, C. E.; Xue, M.; Carnes, E. C.; Zink, J. I.; Brinker, C. J. Mesoporous Silica Nanoparticle Nanocarriers: Biofunctionality and Biocompatibility. *Acc. Chem. Res.* **2013**, *46*, 792–801.

31 Lee, J. E.; Lee, N.; Kim, T.; Kim, J.; Hyeon, T. Multifunctional Mesoporous Silica Nanocomposite Nanoparticles for Theranostic Applications. *Acc. Chem. Res.* **2011**, *44*, 893–902.

32 Lin, C. X.; Qiao, S. Z.; Yu, C. Z.; Ismadji, S.; Lu, G. Q. Periodic mesoporous silica and organosilica with controlled morphologies as carriers for drug release. *Microporous Mesoporous Mater* **2009**, *117*, 213–219.

33 Chen, Y.; Yin, Q.; Ji, X. F.; Zhang, S. J.; Chen, H. R.; Zheng, Y. Y.; Sun, Y.; Qu, H. Y.; Wang, Z.; Li, Y. P.; Wang, X.; Zhang, K.; Zhang, L. L.; Shi, J. L. Manganese oxide-based multifunctionalized mesoporous silica nanoparticles for pH-responsive MRI, ultrasonography and circumvention of MDR in cancer cells. *Biomaterials* **2012**, *33*, 7126–7137.

34 Chen, Y.; Chen, H. R.; Zhang, S. J.; Chen, F.; Sun, S. K.; He, Q. J.; Ma, M.; Wang, X.; Wu, H. X.; Zhang, L. X.; Zhang, L. L.; Shi, J. L. Structure-property relationships in manganese oxide - nnesoporous silica nanoparticles used for T-1-weighted MRI and simultaneous anticancer drug delivery. *Biomaterials* **2012**, *33*, 2388–2398.

35 Wang, X.; Chen, H. R.; Chen, Y.; Ma, M.; Zhang, K.; Li, F. Q.; Zheng, Y. Y.; Zeng, D. P.; Wang, Q.; Shi, J. L. Perfluorohexane-Encapsulated Mesoporous Silica Nanocapsules as Enhancement Agents for Highly Efficient High Intensity Focused Ultrasound (HIFU). *Adv. Mater.* **2012**, *24*, 785–791.

36 Chen, Y.; Chen, H. R.; Sun, Y.; Zheng, Y. Y.; Zeng, D. P.; Li, F. Q.; Zhang, S. J.; Wang, X.; Zhang, K.; Ma, M.; He, Q. J.; Zhang, L. L.; Shi, J. L. Multifunctional Mesoporous Composite Nanocapsules for Highly Efficient MRI-Guided High-Intensity Focused Ultrasound Cancer Surgery. *Angew. Chem., Int. Ed.* **2011**, *50*, 12505–12509.

37 Wang, X.; Chen, H.; Zheng, Y.; Ma, M.; Chen, Y.; Zhang, K.; Zeng, D.; Shi, J. Au-nanoparticle coated mesoporous silica nanocapsule-based multifunctional platform for ultrasound mediated imaging, cytoclasis and tumor ablation. *Biomaterials* **2013**, *34*, 2057–2068.

38 Shi, J. On the Synergetic Catalytic Effect in Heterogeneous Nanocomposite Catalysts. *Chem. Rev.* **2012**, *113*, 2139–2181.

39 Liu, J.; Qiao, S. Z.; Chen, J. S.; Lou, X. W.; Xing, X. R.; Lu, G. Q. Yolk/shell nanoparticles: new platforms for nanoreactors, drug delivery and lithium-ion batteries. *Chem. Commun.* **2011**, *47*, 12578–12591.

40 Liu, J.; Yang, H. Q.; Kleitz, F.; Chen, Z. G.; Yang, T. Y.; Strounina, E.; Lu, G. Q.; Qiao, S. Z. Yolk-Shell Hybrid Materials with a Periodic Mesoporous Organosilica Shell: Ideal Nanoreactors for Selective Alcohol Oxidation. *Adv. Funct. Mater.* **2012**, *22*, 591–599.

41 Yang, Y.; Liu, X.; Li, X. B.; Zhao, J.; Bai, S. Y.; Liu, J.; Yang, Q. H. A Yolk-Shell Nanoreactor with a Basic Core and an Acidic Shell for Cascade Reactions. *Angew. Chem., Int. Ed.* **2012**, *51*, 9164–9168.